Cellular and Molecular Biology
E-ISSN : 1165-158X / P-ISSN : 0145-5680
www.cellmolbiol.org

# Effects of estrogen on proliferation and apoptosis of osteoblasts through regulating GPER/AKT pathway

Yang Zhang#, Tianlong Jiang#, Shenghui Ni, Wenbo Liu, Peng Luo, Shimin Hao, Penghao Wang, Lei Guo*

Department of Orthopedic Surgery, First Affiliated Hospital, China Medical University, Shenyang, 110001, China

# These authors contributed equally to this work

**ARTICLE INFO**

***Original paper***

***Article history:***
*Received: December 12, 2022*
*Accepted: March 15, 2022*
*Published: June 30, 2022*

***Keywords:***

*Estrogen; Osteoblasts; Autophagy; Apoptosis.*

**ABSTRACT**

This experiment was carried out to study the effects of estrogen on the proliferation and apoptosis of osteoblasts through regulating the G protein-coupled estrogen receptor (GPER)/protein kinase B (AKT) pathway. For this aim, osteoblasts were cultured *in vitro* and divided into control group, estrogen group and inhibitor group after passage. The osteoblasts in the control group were cultured normally, estrogen intervention was made in the estrogen group and G15 inhibitor intervention was made in the inhibitor group. After intervention for 24 h, osteoblasts were collected for detection. The positive expression of GPER and the double-positive expression of Tom20/Lamp2 were detected via immunofluorescence assay. The protein expressions of GPER, AKT and phosphorylated (p)-AKT were detected via Western blotting. The mRNA expression of GPER was detected via qPCR. Moreover, the autophagosomes were observed under a transmission electron microscope, and the apoptosis and cell proliferation were detected via terminal deoxynucleotidyl transferase-mediated dUTP nick end labeling (TUNEL) assay and cell counting kit-8 (CCK8) assay, respectively. Results of the immunofluorescence assay revealed that the positive expression of GPER in the estrogen group was higher than that in the control group and inhibitor group ($p<0.05$), while the double-positive expression of Tom20/Lamp2 in the estrogen group was lower than that in control group and inhibitor group ($p<0.05$). According to the results of Western blotting, the relative protein expression of AKT had no differences among the three groups ($p>0.05$), while the relative protein expressions of GPER and p-AKT in the estrogen group were higher than those in the control group and inhibitor group ($p<0.05$). The results of qPCR showed that the relative mRNA expression of GPER in the estrogen group was higher than that in the control group and inhibitor group ($p<0.05$). There were a small number of autophagosomes in osteoblasts in the control group and inhibitor group, while the number of autophagosomes in osteoblasts was smaller in the estrogen group. Besides, the estrogen group had a remarkably lower apoptosis rate of osteoblasts than the control group and inhibitor group and a remarkably higher proliferation rate than the control group and inhibitor group. Then estrogen can inhibit the mitochondrial autophagy of osteoblasts by regulating the GPER/AKT pathway, thereby inhibiting apoptosis and promoting cell proliferation.

**Doi:** http://dx.doi.org/10.14715/cmb/2022.68.6.20 

## Introduction

Postmenopausal osteoporosis (PMO) is one of the important diseases of the perimenopausal syndrome, which frequently occurs in menopausal women aged about 50 years old, characterized by a high clinical morbidity rate and persistent pain (1, 2). It is currently believed that the onset of PMO is closely related to the fact that the weakening of ovarian function due to ovary degeneration leads to metabolic disorders of the endocrine system, thus affecting bone metabolism. As a major perimenopausal syndrome, PMO often causes persistent pain and fractures, and even disability or death in patients (3, 4). Therefore, research on the pathogenesis of PMO and its related treatment is urgently needed.

Estrogen and osteoblasts play important roles in the pathogenesis of PMO. Currently, research suggests that estrogen deficiency and a decrease in osteoblasts are important factors in the occurrence of PMO. On the one hand, estrogen deficiency can lead to changes in the cytokine network system that regulates the production of osteoclasts and osteoblasts. On the other hand, postmenopausal estrogen deficiency can aggravate the autophagy of osteoblasts, leading to apoptosis of a large number of osteoblasts. Therefore, there is a close correlation between estrogen deficiency and the increased degree of apoptosis of postmenopausal osteoblasts. Increasingly more in vivo and in vitro experiments have demonstrated that estrogen can protect osteoblasts and prevent and treat osteoporosis (5). However, the molecular biological mechanism of estrogen in protecting osteoblasts from injury remains unclear. The biological effects of estrogen are mainly mediated by estrogen receptors, one of which is the G protein-coupled estrogen receptor (GPER) (6, 7). Estrogen

* Corresponding author. Email: guolei2022@yandex.com

can bind to estrogen receptors, thereby regulating the physiological functions of various systems in the body (8, 9). In addition, the phosphatidylinositol 3-hydroxy kinase (PI3K)/protein kinase B (AKT) signaling pathway is a ubiquitous and important intracellular signal transduction pathway, which is closely related to cell proliferation, differentiation, apoptosis and autophagy. Therefore, it is of important significance to study the effects of estrogen on the proliferation and apoptosis of osteoblasts from the GPER and PI3K/AKT signaling pathways.

Therefore, the present study aims to explore the effects of estrogen on the proliferation and apoptosis of osteoblasts through the GPER/AKT pathway, and further determine the important role of estrogen in the pathological process of osteoporosis and its mechanism of action.

## Materials and Methods

### Laboratory cells

The mouse MC3T3-E1 osteoblasts were purchased from Nanjing COBIOER Co., Ltd.

### Laboratory reagents and instruments

Dulbecco's modified Eagle medium (DMEM) (Hyclone, USA), fetal bovine serum (FBS) (Hyclone, USA), estrogen (Sigma-Aldrich, USA), GPER inhibitor G15 (Tocris, USA), primary antibodies: anti-GPER antibody (Abcam, USA) and anti-AKT/phosphorylated (p)-AKT antibody (Abcam, USA), secondary antibodies: IFKine donkey anti-rabbit immunoglobulin G (IgG) fluorescence secondary antibody (Abbkine, USA), IFKine donkey anti-goat IgG (Abbkine, USA), horseradish peroxidase-labeled goat anti-rabbit IgG (Beyotime, Hangzhou), horseradish peroxidase-labeled donkey anti-goat IgG (Beyotime, Hangzhou), horseradish peroxidase-labeled goat anti-mouse IgG (Beyotime, Hangzhou), AceQ quantitative polymerase chain reaction (qPCR) SYBR Green Master Mix Kit (Vazyme, Nanjing), HiScript II Q RT SμperMix for qPCR (+gDNA wiper) kit (Vazyme, Nanjing), optical microscope (Leica DMI 4000B/DFC425C, Germany), fluorescence qPCR instrument (ABI 7500, USA), and Image-Pro image analysis system (BIORADHERCULES, USA).

### Cell culture

After resuscitation, the mouse MC3T3-E1 osteoblasts were added with a complete DMEM/F12 medium containing 5% FBS, and the cell concentration was adjusted, followed by culture in an incubator with 5% $CO_2$ at 37°C. The medium was replaced once every 3 d, and the cell growth was closely observed, followed by passage when 80-90% of cells were fused. Then the cell concentration was adjusted, and the cells continued to be cultured in the culture dish at an appropriate concentration. The cells were used for experiments when passaged till the third generation.

### Cell grouping and treatment

After cell digestion, the cell concentration was adjusted, and the cells were inoculated into a 96-well plate ($5\times10^4$ cells/mL) in the incubator with 5% $CO_2$ at 37°C. On the next day, MC3T3-E1 osteoblasts were randomly divided into the control group, estrogen group and inhibitor group. In the control group, the cells were normally cultured in vitro without any treatment and collected for detection after 24 h. In the estrogen group, $10^{-7}$ M of estrogen was added into the medium for intervention, and the cells were collected for detection after 24 h. In the inhibitor group, $10^{-7}$ M of estrogen and 15 μM of inhibitor G15 were added into the medium for intervention, and the cells were collected for detection after 24 h.

### Immunofluorescence detection of positive expression of GPER and double-positive expression of Tom20/Lamp2

After the intervention, the medium was removed, and the cells were fixed with 4% paraformaldehyde solution for 15 min. After washing to remove the paraformaldehyde solution, Triton X-100 at a concentration of 0.1% was added for transparentization. After washing, the cells were sealed with BSA in each well. Then the sealing buffer was discarded, and the cells were incubated with the GPER primary antibody (1:50) solution or a mixture of Tom20 (1:50) and Lamp2 (1:50) primary antibodies in a wet box at 4°C overnight. After rewarming on the next day, the primary antibodies were washed away, and the diluted fluorescence secondary antibody (1:1000) solution was added dropwise for a reaction for 1 h, followed by washing. Finally, DAPI solution was added dropwise for a reaction for 3 min in a dark place, and the cells were washed, sealed and observed under a fluorescence microscope.

### Detection of protein expression via Western blotting

The cells were added with lysis buffer and subjected to ice bath for 1 h and centrifugation in a centrifuge at 14,000 g for 10 min. The protein was quantified using the BCA method. The absorbance of protein was detected using a microplate reader and the standard curve was plotted, based on which the protein concentration was calculated. After protein denaturation, the protein in cells was separated via SDS-PAGE, and the position of the Marker protein was observed. The electrophoresis was terminated when the Marker protein reached the bottom of the glass plate in a straight line. Then the protein was transferred onto a PVDF membrane, sealed with the sealing buffer for 1.5 h and incubated with the anti-GPER (1:1000), anti-AKT (1:1000) and anti-p-AKT (1:1000) primary antibodies and secondary antibodies (1:1000). After the membrane was washed, the image was fully developed using the chemiluminescent reagent for 1 min.

The total RNA was extracted from cells and reversely transcribed into cDNA using the reverse transcription kit. The qPCR system (20 μL) was designed and the reaction conditions are as follows: reaction at 51°C for 2 min, predenaturation at 96°C for 10 min, denaturation at 96°C for 10 s and annealing at 60°C for 30 s, for a total of 40 cycles. With GAPDH as an internal reference, the relative mRNA expression was calculated. The primer sequences are shown in Table 1.

**Table 1.** Primer sequences.

| Gene | Primer sequence |
|---|---|
| GPER | F: 5'-AACAGAGCAGCGATCTGGAC-3'<br>R: 5'-GCAGAGTCCTTGGATGGCTT-3' |
| GAPDH | F: 5'-ACGGCAAGTTCAACGGCACAG-3'<br>R: 5'-GAAGACGCCAGTAGACTCCACGAC-3' |

### Observation of autophagosome formation under a transmission electron microscope

After intervention, the cells were fixed with glutaraldehyde fixative at a concentration of 2.5% in a refrigerator at 4°C overnight. After washing on the next day, the cells were fixed again with osmic acid at a concentration of 1% for 1 h, followed by washing, dehydration, complete immersion and embedding. Then the embedding block was sliced into 70-90 nm-thick sections, stained with uranyl acetate (saturated solution of 50% ethanol) for 15 min and lead citrate solution for 15 min, and observed under the transmission electron microscope.

### Detection of apoptosis via terminal deoxynucleotidyl transferase-mediated dUTP nick end labeling (TUNEL) assay

The cells were collected and fixed with 4% paraformaldehyde for 30 min, followed by a reaction with proteinase K at room temperature for 15 min according to the instructions of the TUNEL assay kit. After the cells were washed with PBS, sealing buffer was added for reaction at room temperature for 10 min, and the cells were washed again with PBS, followed by a labeling reaction. Finally, the reaction solution was added dropwise for a reaction for 10 min, and the cells were washed and observed.

### Detection of cell proliferation via CCK8 assay

The cells in each group were uniformly inoculated into the 96-well plate and cultured in the incubator for 24 h. CCK8 solution was added into each well according to the instructions of the CCK8 kit, followed by incubation in the incubator for 1 h. Then the optical density (OD) value was measured at 450 nm using a microplate reader, based on which the cell proliferation rate was calculated.

### Statistical methods

In this study, SPSS 20.0 software was used for statistical analysis. Enumeration data were expressed as mean ± standard deviation. *t* test was used for the data in line with normal distribution and homogeneity of variance, corrected *t* test for the data in line with normal distribution and heterogeneity of variance, and non-parametric test for the data not in line with normal distribution and homogeneity of variance. Rank sum test was adopted for ranked data, and chi-square test was adopted for enumeration data.

## Results

### GPER expression detected via an immunofluorescence assay

As shown in Figure 1, the positive expression of GPER showed a red color mainly in the cytoplasm. According to the statistical results (Figure 2), the number of GPER-positive cells was significantly increased in the estrogen group compared with that in the control group and inhibitor group, showing statistically significant differences ($p<0.05$), while it had no significant difference between control group and inhibitor group ($p>0.05$).

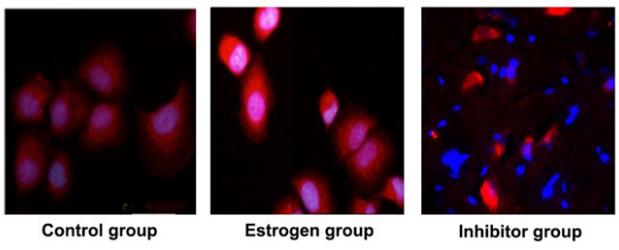


**Figure 1.** GPER positive expression detected via immunofluorescence assay (×200).

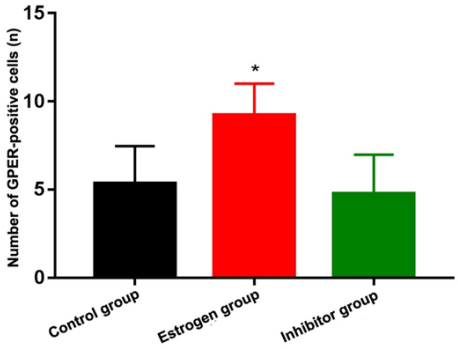


**Figure 2.** Number of GPER-positive cells in each group. Note: *$p<0.05$ vs. control group and inhibitor group.

### Double-positive expression of Tom20/Lamp2 detected via an immunofluorescence assay

As shown in Figure 3, the positive expression of Tom20 and Lamp2 displayed the red and green color, respectively,

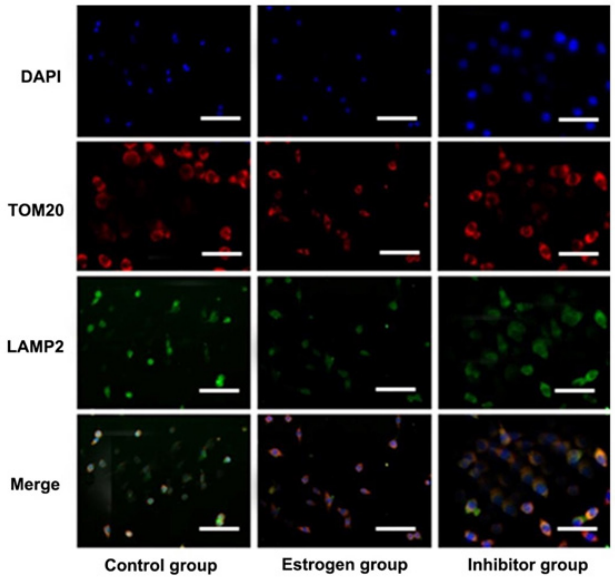


**Figure 3.** Tom20/Lamp2 double-positive expression detected via immunofluorescence assay (×200)

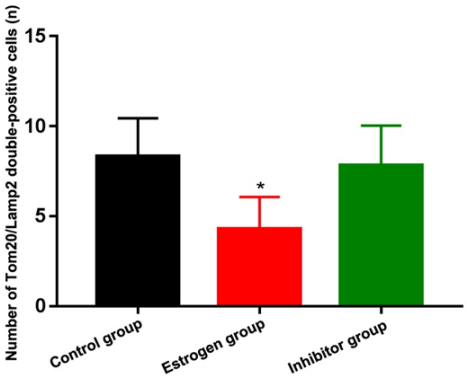


**Figure 4.** Number of Tom20/Lamp2 double-positive cells in each group. Note: *$p<0.05$ vs. control group and inhibitor group.

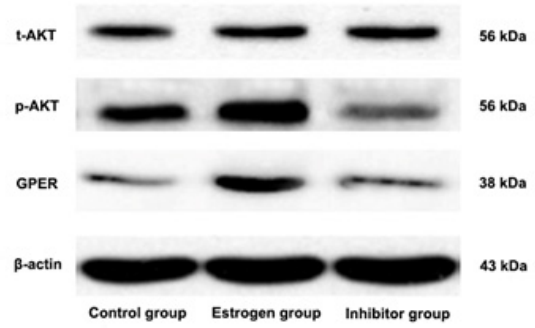


**Figure 5.** Protein expressions detected via Western blotting.

while the double-positive expression of Tom20/Lamp2 displayed the yellow color mainly in the cytoplasm. According to the statistical results (Figure 4), the number of Tom20/Lamp2 double-positive cells was decreased in the estrogen group compared with that in the control group and inhibitor group, showing statistically significant differences ($p$<0.05), while it had no obvious difference between control group and inhibitor group ($p$>0.05).

### Related protein expressions detected via Western blotting

As shown in Figure 5, the protein expressions of GPER and p-AKT were higher in the estrogen group and lower in the control group and inhibitor group. According to the statistical results (Figure 6), the relative protein expressions of GPER and p-AKT were remarkably increased in the estrogen group compared with those in the control group and inhibitor group, and the differences were statistically significant ($p$<0.05). The relative protein expressions of GPER and p-AKT had no significant differences between the control group and the inhibitor group ($p$>0.05). Besides, no differences were found in the relative protein expression of t-AKT among the three groups ($p$<0.05).

### GPER mRNA expression detected via qPCR

The estrogen group had a remarkably higher mRNA expression level of GPER than the control group and inhibitor group, displaying statistically significant differences ($p$<0.05), while the mRNA expression level of GPER had no remarkable difference between the control group and inhibitor group ($p$>0.05) (Figure 7).

### Autophagosomes observed under the transmission electron microscope

In the control group, the morphology of the nucleus, cytoplasm and organelle was normal in MC3T3-E1 osteoblasts, and a small number of autophagic vesicles were observed in the cytoplasm. In the estrogen group, the number of autophagic vesicles in the cytoplasm significantly declined in MC3T3-E1 osteoblasts. In the inhibitor group, the morphology of MC3T3-E1 osteoblasts was similar to that in the control group (Figure 8).

### Apoptosis detected via TUNEL assay

The apoptosis rate remarkably declined in the estrogen group compared with that in the control group and inhibitor group, displaying statistically significant differences ($p$<0.05), while it had no obvious difference between the control group and inhibitor group ($p$>0.05) (Figure 9).

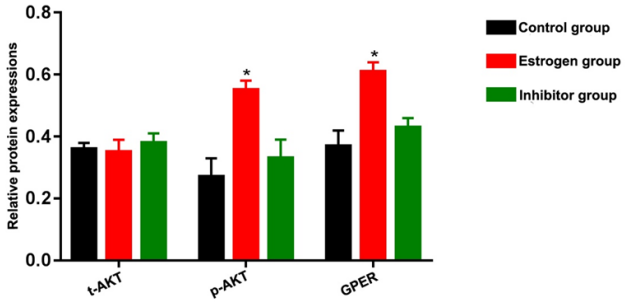


**Figure 6.** Relative protein expressions in each group. Note: *$p$<0.05 vs. control group and inhibitor group.

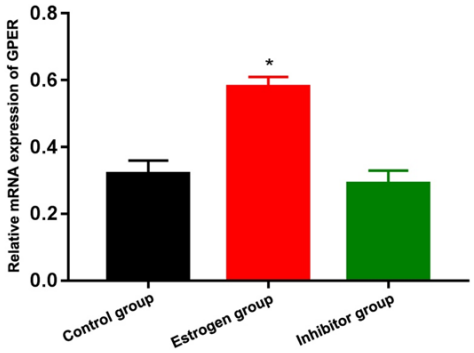


**Figure 7.** Relative mRNA expression of GPER in each group. Note: *$p$<0.05 vs. control group and inhibitor group.

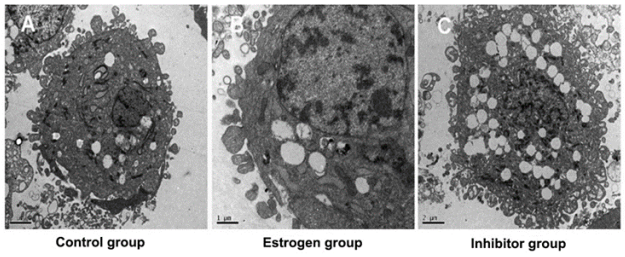


**Figure 8.** Autophagosomes observed under the transmission electron microscope.

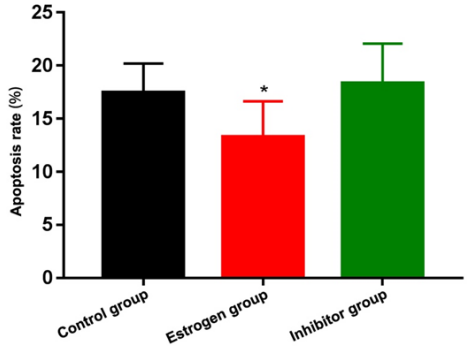


**Figure 9.** Apoptosis rate in each group. Note: *$p$<0.05 vs. control group and inhibitor group.

### Cell proliferation detected via CCK8 assay

The cell proliferation rate was evidently increased in the estrogen group compared with that in the control group and inhibitor group, displaying statistically significant differences ($p$<0.05), while it had no evident difference between the control group and the inhibitor group

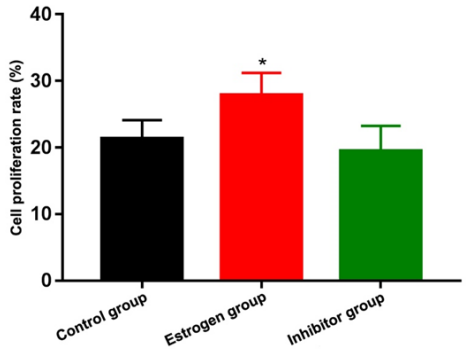


**Figure 10.** Cell proliferation rate in each group. Note: $^{*}p<0.05$ vs. control group and inhibitor group.

($p>0.05$) (Figure 10).

## Discussion

Currently, it is believed that the pathogenesis of PMO is that the decline in ovarian function in elderly postmenopausal women leads to insufficient secretion of estrogen, thus affecting the bone metabolism and causing significantly more bone loss than bone formation, ultimately increasing bone fragility and damaging the internal structure of bone tissues over time (9, 10). The most common clinical symptoms of PMO are persistent pain and malformation and fracture due to increased fragility and damage to bone tissues, which affects cardiopulmonary function in severe cases. In particular, the fracture and malformation caused by PMO result in immobilization of patients, seriously affecting their living quality and even causing death in patients. The main pathogenesis of PMO in postmenopausal women is estrogen deficiency, leading to changes in the cytokine network system that regulates the production of osteoclasts and osteoblasts. Increasingly *in vivo* and in vitro experiments have demonstrated that estrogen can protect osteoblasts and prevent and treat osteoporosis (5). A study has shown that estrogen can activate GPER to exert its physiological functions in myocardial cells and cancer cells (11). In the present study, mRNA and protein expressions of GPER were found in mouse MC3T3-E1 osteoblasts, suggesting that estrogen may also play a role through GPER in MC3T3-E1 osteoblasts. In addition, it was observed under the immunofluorescence microscope that estrogen could obviously promote the protein expression of GPER in osteoblasts. Moreover, the high-affinity specific inhibitor G15 of GPER could block the promoting effect of estrogen on mRNA and protein expressions of GPER, further indicating that estrogen can regulate both relative mRNA and protein expressions of GPER in osteoblasts.

As one of the important organelles of cells, the mitochondrion is considered as the power of cells, involved in important pathophysiological processes, such as cell survival and death (12). After the oxidative stress response causes mitochondrial damage, mitochondrial autophagy will be activated to eliminate the damaged mitochondria. Autophagy is an important pathophysiological response, which is a "double-edged sword" for cells and organisms (13, 14). It can be said that autophagy controls cell fate by regulating apoptosis, and excessive autophagy will aggravate apoptosis, harming cell proliferation. According to a recent study, the protective effect of estrogen on nerve cells may be realized by regulating the degree of autophagy (15). In the present study, it was found under the transmission electron microscope that estrogen could lower the number of autophagic vesicles in osteoblasts, and reduce the number of Tom20/Lamp2 double-positive cells, namely the mitochondrial autophagosomes, indicating that estrogen can suppress mitochondrial autophagy in mouse MC3T3-E1 osteoblasts. In addition, the high-affinity specific inhibitor G15 of GPER could block the decline in the number of mitochondrial autophagosomes induced by estrogen, suggesting that estrogen can inhibit mitochondrial autophagy in mouse MC3T3-E1 osteoblasts through GPER, which may be one of the causes and mechanisms of the significant decrease in apoptosis rate and significant increase in cell proliferation rate in estrogen group.

The PI3K/AKT signaling pathway is an important intracellular signaling pathway, as well as one of the important signaling pathways regulating autophagy, which can exert an important inhibitory effect on autophagy (16). After the injury, the PI3K/AKT signaling pathway can be effectively activated by various cytokines and stress responses, and the important key molecules such as AKT in this pathway are phosphorylated, thereby inhibiting autophagy (17). The results in the present study revealed that estrogen facilitated the phosphorylation of AKT protein in MC3T3-E1 osteoblasts, thus activating the above signaling pathway, while GPER-specific inhibitor G15 could counteract the negative effect of estrogen on mitochondrial autophagy in MC3T3-E1 osteoblasts. At the same time, considering the effect of estrogen on GPER, these results demonstrate that estrogen inhibits mitochondrial autophagy through the GPER-mediated PI3K/AKT signaling pathway, thereby inhibiting apoptosis and facilitating cell proliferation.

In conclusion, estrogen can inhibit the mitochondrial autophagy of osteoblasts by regulating the GPER/AKT pathway, thus suppressing apoptosis and promoting cell proliferation.

## Acknowledgments
Not applicable.

## Interest conflict
The authors declare that they have no conflict of interest.

## Fundings
The research is supported by: This work was supported by the National Natural Science Foundation of China (No. 81971322), the Natural Science Foundation of Liaoning Province (No. 20170541033).

## References

1. Wang Q, Li Y, Zhang Y, et al. LncRNA MEG3 inhibited osteogenic differentiation of bone marrow mesenchymal stem cells from postmenopausal osteoporosis by targeting miR-133a-3p. Biomed Pharmacother 2017; 89:1178-1186.
2. Aursnes I, Storvik G, G Semyr J. A Bayesian analysis of bisphosphonate effects and cost-effectiveness in post-menopausal osteoporosis. Pharmacoepidemiol Drug Saf 2000; 9(6):501-509.
3. Paschalis E P, Gamsjaeger S, Hassler N. Vitamin D and calcium supplementation for three years in postmenopausal osteoporosis significantly alters bone mineral and organic matrix quality. Bone

2017; 95:41-46.
4. Mignot M A, Taisne N, Legroux I, Cortet B, Paccou J. Bisphosphonate drug holidays in postmenopausal osteoporosis: effect on clinical fracture risk. Osteoporos Int 2017; 28(12): 1-8.
5. Sadat-Ali M, Elq A H A, Al-Turki H A. Influence of vitamin D levels on bone mineral density and osteoporosis. Ann Saudi Med 2011; 31(6):602-608.
6. Zhou L, Zhang J, Wang C, Sun Q. Tanshinone inhibits neuronal cell apoptosis and inflammatory response in cerebral infarction rat model. Int J Immunopathol Pharmacol 2017; 30(2): 123-129.
7. Ji J F, Ma X H. Effect of baculovirus P35 protein on apoptosis in brain tissue of rats with acute cerebral infarction. Genet Mol Res 2015; 14(3): 9353-9360.
8. Yang Z, Klionsky D J . Eaten alive: a history of macroautophagy. Nat Cell Biol 2010; 12(9):814-822.
9. Hung C C, Davison E J, Robinson P A. The aggravating role of the ubiquitin-proteasome system in neurodegenerative disease. Biochem Soc Trans 2006; 34(5):743-745.
10. Tella S H, Kommalapati A, Correa R. Profile of Abaloparatide and Its Potential in the Treatment of Postmenopausal Osteoporosis. Cureus 2017; 9(5): e1300.
11. Cano A, Chedraui P, Goulis D G, et al. Calcium in the prevention of postmenopausal osteoporosis: EMAS clinical guide. Maturitas 2018; 107:7-12.
12. Yang W, Tan W, Zheng J. MEHP promotes the proliferation of cervical cancer via GPER mediated activation of AKT. Euro J Pharmacol 2018; 824:11-16.
13. Kim J A, Wei Y, Sowers J R. Role of mitochondrial dysfunction in insulin resistance. Circ Res 2008; 102(4): 401-414.
14. Chen W, Sun Y, Liu K. Autophagy: A double-edged sword for neuronal survival after cerebral ischemia. Neural Regen Res 2014; 9(12):1210-1216.
15. Zhang S J, Yang W, Wang C. Autophagy: A double-edged sword in intervertebral disc degeneration. Clin Chim Acta 2016; 457:27-35.
16. Tsujimoto Y, Shimizu S . Another way to die: autophagic programmed cell death. Cell Death Differ 2005; 12:1528-1534.
17. Lin C W, Chen B, Huang K L. Inhibition of Autophagy by Estradiol Promotes Locomotor Recovery after Spinal Cord Injury in Rats. Neurosci Bull 2016; 32(2):137-144.
18. Kimura S, Fujita N, Noda T. Monitoring autophagy in mammalian cultured cells through the dynamics of LC3. Methods Enzymol 2008; 452:1-12.
19. Kroemer G, Marino G, Levine B. Autophagy and the integrated stress response. Mol Cell 2010; 40(2): 280-293.
20. Antoon J W, Bratton M R, Guillot L M. Inhibition of p38-MAPK alters SRC coactivation and estrogen receptor phosphorylation. Cancer Biol Ther 2012; 13(11):1026-1033.